

**Acoustic Emission-based crack tracking for existing concrete structures  
Influence of number of load cycles and loading speed**

Zhang, F.; Yang, Y.; Hendriks, M.A.N.

**DOI**

[10.1201/9780429279119-327](https://doi.org/10.1201/9780429279119-327)

**Publication date**

2021

**Document Version**

Final published version

**Published in**

Bridge Maintenance, Safety, Management, Life-Cycle Sustainability and Innovations

**Citation (APA)**

Zhang, F., Yang, Y., & Hendriks, M. A. N. (2021). Acoustic Emission-based crack tracking for existing concrete structures: Influence of number of load cycles and loading speed. In H. Yokota, & D. M. Frangopol (Eds.), *Bridge Maintenance, Safety, Management, Life-Cycle Sustainability and Innovations: Proceedings of the Tenth International Conference on Bridge Maintenance, Safety and Management (IABMAS 2020)* (1st ed., pp. 2393-2399). CRC Press. <https://doi.org/10.1201/9780429279119-327>

**Important note**

To cite this publication, please use the final published version (if applicable).  
Please check the document version above.

**Copyright**

Other than for strictly personal use, it is not permitted to download, forward or distribute the text or part of it, without the consent of the author(s) and/or copyright holder(s), unless the work is under an open content license such as Creative Commons.

**Takedown policy**

Please contact us and provide details if you believe this document breaches copyrights.  
We will remove access to the work immediately and investigate your claim.

***Green Open Access added to TU Delft Institutional Repository***

***'You share, we take care!' - Taverne project***

**<https://www.openaccess.nl/en/you-share-we-take-care>**

Otherwise as indicated in the copyright section: the publisher is the copyright holder of this work and the author uses the Dutch legislation to make this work public.

# Acoustic Emission-based Crack Tracking for Existing Concrete Structures: Influence of Number of Load Cycles and Loading Speed

F. Zhang<sup>a</sup>, Y. Yang<sup>a</sup> & M.A.N. Hendriks<sup>a,b</sup>

<sup>a</sup>*Delft University of Technology, Delft, the Netherlands*

<sup>b</sup>*Norwegian University of Science and Technology, Trondheim, Norway*

**ABSTRACT:** Acoustic Emission (AE)-based crack tracking is a promising approach to locate the cracks in concrete structures. Different from conventional AE, this approach uses AE activities during crack closure. But, AE activities during crack closure may be influenced by number of load cycles and loading speed. This may challenge the applicability of AE-based crack tracking, especially for existing concrete structures with many load cycles in the service life. This paper investigated the influence of number of load cycles and loading speed on AE-based crack tracking. A total of 80 load cycles were applied on a pre-cracked concrete beam. The last 5 cycles had increasing loading speeds. AE-based crack tracking was carried out in each load cycle. For calibration, Digital Image Correlation (DIC) was performed to measure the crack opening and closure. We found that AE-based crack tracking can locate the cracks, while, with many load cycles, it cannot indicate the crack width. Loading speed had little influence on AE-based crack tracking. The results of this paper suggested the applicability of AE-based crack tracking for existing concrete structures.

## 1 INTRODUCTION

Existing concrete structures require effective crack detection for safety assessment (Soutsos et al., 2012). But, visual inspection and traditional displacement measurements like LVDTs are not always possible, especially when access to the interest volume is restricted (like internal cracks) (fib, 2003). Acoustic Emission (AE) monitoring is a solution by detecting elastic waves from cracking either inside or on the surface of the concrete structures using AE sensors (Muralidhara et al., 2009, Schechinger and Vogel, 2007). Conventional AE monitoring requires heavy loading to open new cracks or further develop the existing cracks. However, it risks further damaging the structure. Besides, application of heavy loading is expensive. An alternative approach, in which cyclic loading with relatively low magnitude is applied, has been recently proposed (Zhang and Yang, 2019). Existing cracks are opened and closed during a load cycle. AE activities during crack closure are used to track the trajectory of the cracks. This approach is called AE-based crack tracking. The lab tests show that AE based crack tracking agrees with the crack patterns for concrete specimens.

However, existing concrete structures such as concrete bridges underwent many load cycles before the time of test. With more load cycles, cracks were

opened and closed more times. In this process, the AE activities during crack closure, which are used in AE-based crack tracking, may be influenced. Therefore, we need to clarify the influence of number of load cycles on AE-based crack tracking.

In addition, influence of loading speed on AE-based crack tracking is unclear. Lantsoght et al. found that loading speed from 0.004 mm/s to 0.4 mm/s was irrelevant to the structural stiffness in proof load testing (Lantsoght et al., 2017). But, few researches relate the loading speed to the AE activities during crack closure that are used in AE-based crack tracking.

The goal of this paper is to investigate the influence of number of load cycles and loading speed on AE based crack tracking. We applied a total of 80 load cycles on a pre-cracked concrete beam with the same magnitude. The last 5 load cycles had increasing loading speeds. AE-based crack tracking was performed in each load cycle. In the meantime, Digital Image Correlation (DIC) was applied to measure the crack opening and closure. By comparing the results of AE based crack tracking with DIC in different cycles, we evaluated the performance of AE-based crack tracking influenced by number of load cycles and loading speed. Finally, we gave suggestions on applying AE based crack tracking in existing concrete structures.

## 2 AE-BASED CRACK TRACKING

AE activities have been observed during unloading of concrete structures with cracks (Ohtsu et al., 2002). They mainly come from the contact and/or sliding of the rough crack surfaces during crack closure. Therefore, the locations of the AE activities during crack closure indicate the location of the crack surfaces. This is the basic principle of AE-based crack tracking.

Ohtsu et al. found that, at structural level, AE activities during crack closure were related to the crack opening/closure (Ohtsu et al., 2002). By discretizing the measuring area into cells, AE-based crack tracking links the local cumulative AE activities to the local crack closure at cell level. Thus, AE-based crack tracking can locate the crack and indicate the widths along the crack profile.

The cell size is limited by the source localization error, which is measured as the distance between the estimated and real source locations. The applied source localization algorithm in this study is the grid search method based on arrival times (Grosse and Ohtsu, 2008). Considering the arrival time picking error and the presence of a crack between the source and the receiver, the source localization error for existing concrete structures was found less than 15 cm (Zhang, 2017). In this case, the cell size is suggested no smaller than 15 cm.

## 3 EXPERIMENT

The presented experiment is a part of a larger research program supported by the Dutch ministry of infrastructure and the environment (Zarate Garnica and Yang, 2018). The main goal of the research program is to

evaluate the shear behavior of deep reinforced concrete beam without shear reinforcement.

As a part of the research, AE measurement was employed in a number of tests. Test on beam, which is numbered as H653, investigated the influence of number of load cycles and loading speed on AE-based crack tracking.

### 3.1 Beam configurations

The reinforced concrete beam H653 has a length of 10 m, a height of 1.2 m, and a width of 0.3 m. The nominal compressive strength of the concrete is 65 MPa. The maximum aggregate size is 16 mm. Longitudinal reinforcing bars are 6 $\varnothing$ 25, with concrete cover of 25 mm. The beam was simply supported with a span of 9 m, and loaded by a point load at 3 m from one support (Figure 1).

The loading scheme consisted of 4 stages (Figure 2). In Stage 1, we loaded the beam to 200 kN to open a crack in the measuring zone. The purpose was to reproduce the condition that the existing concrete structure was cracked due to heavier loads before the time of test. Then, we applied 75 repeated load cycles with maximum load of 150 kN (L1-L75 in Stage 2) to investigate the influence of the number of load cycles on AE-based crack tracking. In this Stage, the beam was loaded under displacement-control with a loading speed of 0.02 mm/s. In Stage 3, we applied five load cycles L76-L80 with increasing loading speeds, which were respectively 0.04 mm/s, 0.08 mm/s, 0.16 mm/s, 0.32 mm/s, and 0.64 mm/s. Afterwards, we loaded the beam until failure (Stage 4).

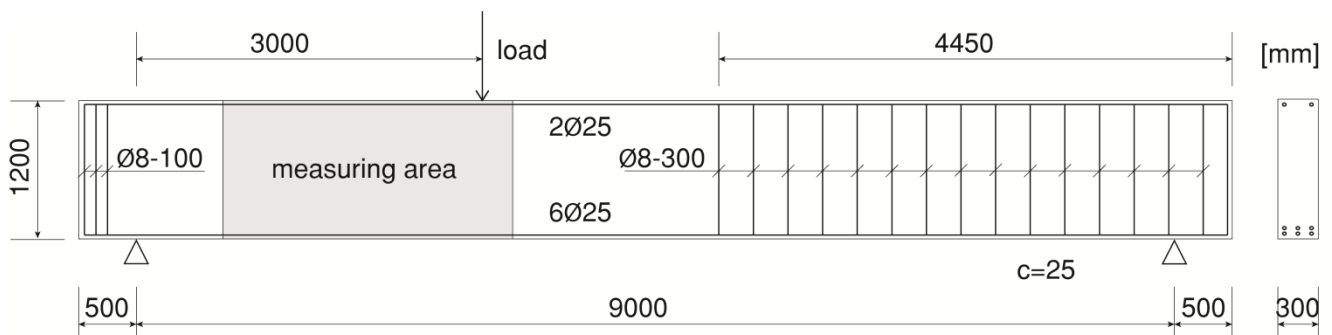


Figure 1. Beam configurations.

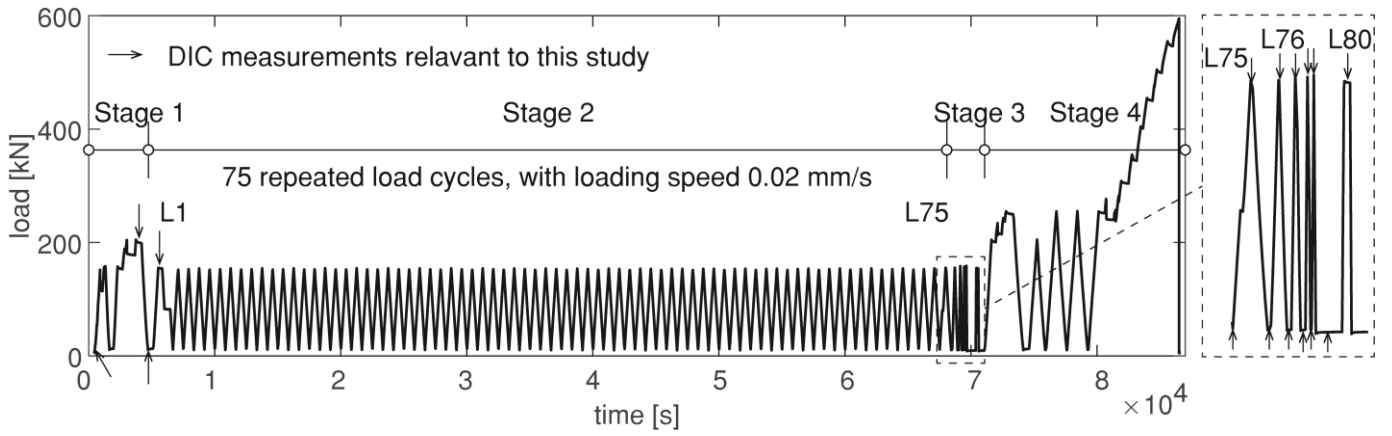


Figure 2. Loading scheme.

### 3.2 AE-based crack tracking

Fifteen AE sensors with a central frequency of 60 kHz (MISTRAS) were installed on the surface of the beam (Figure 3). AE-based crack tracking was performed in loading Stage 2 and Stage 3 (Figure 2). Among all the received AE hits, we used those with peak amplitude larger than 60 dB. The arrival time of an AE hit was recorded as the first point in the signal crossing the threshold of 45 dB. Based on the arrival times, grid search method with grid size of 5 mm was applied to locate AE activities. The located AE activities that were outside the sensor enclosed area were eliminated (Zhang, 2017).

Supposing source localization error less than 15 cm, we discretized the measuring area into cells of 15 cm, then counted the cumulative AE activities in each cell.

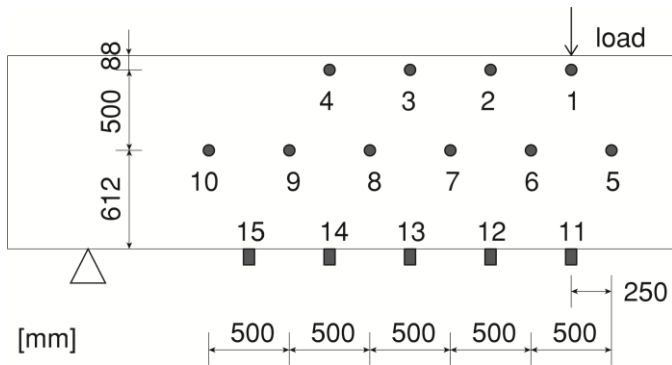


Figure 3. AE sensor layout on one side of the beam.

### 3.3 Measurement of crack profile and closure with DIC

DIC was used for displacement measurement (Zarate Garnica, 2018). A sprinkle pattern was painted on the other surface of the beam opposite to AE (Figure 4). An open source Matlab code was used to do the DIC calculation (Eberl, 2010).

With the displacement field, the crack closure was calculated as the displacement difference be-

tween loaded and unloaded conditions at points along the crack profile. The time of DIC measurement is marked in Figure 2. Note that, for L1 and L80, we can only know the crack opening during loading. Since crack opening and closure in a load cycle was observed comparable (not shown), this paper used crack opening during loading to indicate crack closure during unloading in every load cycle.



Figure 4. Photo of DIC sprinkle pattern on the other side of the beam.

Since the width of the beam was small in relation to its height and length, comparable crack closures were assumed on the two sides of the beam. DIC results were used to calibrate the AE-based crack tracking results.

## 4 RESULTS

### 4.1 Crack pattern

The beam was cracked in loading Stage 1 by a heavier load of 200 kN. We observed 2 major cracks—CR1 and CR2 from DIC (Figure 5a). AE sensors and the cells were projected to the DIC crack pattern. CR1 lied on the edge of the AE measuring area,

where the accuracy of source localization was limited (Zhang, 2017). Therefore, the following study focused on CR2.

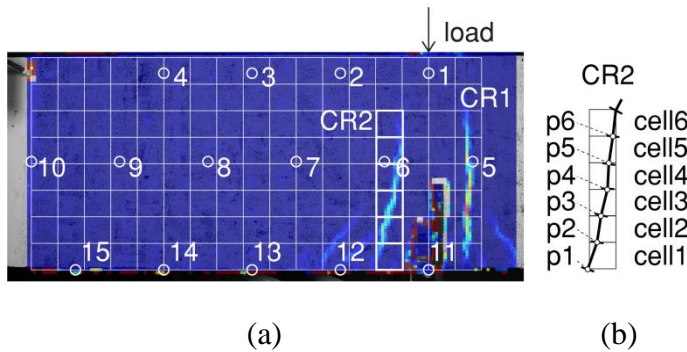


Figure 5. (a) Crack pattern at 200 kN from DIC with the projected AE sensors and cells, (b) local crack closure measuring points (p1-p6) and the AE cells with CR2 (cell1-cell6).

CR2 went through six AE cells (cell1-cell6) (Figure 5b). The local crack closure in these cells were respectively determined at measuring points p1-p6 (marked in Figure 5b) by DIC. Assuming a decreasing crack opening to the crack tip, the measuring point indicated the maximum local crack opening in each cell. In this way, we ignored the variance of local crack profile in each cell.

The local crack closures in L1, L75-L80 are shown in Figure 6. Cell3, which was at height 0.3 m, had the maximum local crack closure. It was reasonable since the crack openings near the bottom of the beam were limited by the bending reinforcements.

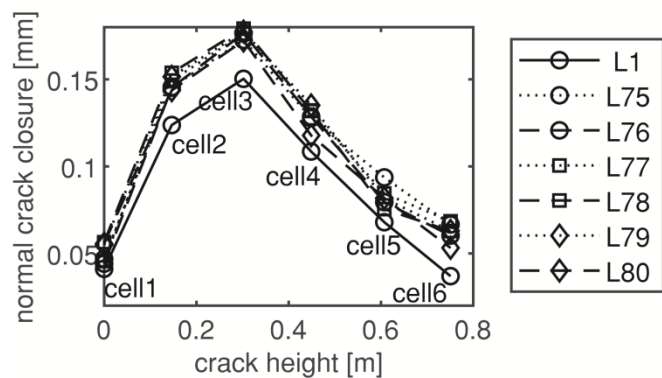


Figure 6. Local crack closure at cell1-cell6.

#### 4.2 Influence of number of load cycles

Comparison of the results in load cycles L1-L75, which had same loading speeds, can reflect the influence of number of load cycles on local crack closure and AE-based crack tracking.

#### Influence of number of load cycles on local crack closure

From Figure 6, we observed a significant increase of local crack closure after 75 load cycles. Local crack closure in cell3, as an example, increased from 0.1503 mm to 0.1726 mm. Considering a compara-

ble crack width when the crack was open, more crack closure indicated less remaining crack width when the crack was (partially) closed, which was possibly related to the smoother of crack surfaces after more load cycles.

#### Influence of number of load cycles on AE-based crack tracking

The total AE activities decreased with the increasing number of load cycles (see Figure 7). Crack surfaces were expected to be smoother due to more load cycles. Thus, the closure of smoother crack surfaces generated less AE activities.

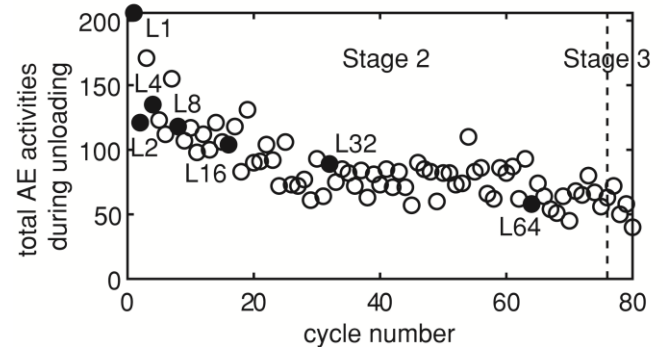


Figure 7. Total AE activities during unloading in each load cycle in loading Stage 2 and Stage 3, with black points selected as examples to show the source localization results.

Figure 8 shows the local cumulative AE activities in the selected load cycles (marked as black points in Figure 7). The left side shows the original AE source localization results, and the right side shows the map of local cumulative AE activities in cells. Location of CR2 was projected to the map of local cumulative AE activities. Though original AE source localization results can indicate the crack location with certain accuracy, they couldn't quantitatively show the density of AE activities in a local area. Instead, AE-based crack tracking, which produced map of local cumulative AE activities, can quantify the spatial distribution and carry out local study.

With increasing number of load cycles, the crack location can be estimated, though the magnitude of local cumulative AE activities decreased.

We also found that AE activities were not only located in the cells with CR2. AE in the cells near the bottom reinforcements could come from the closure of secondary cracks, slip between reinforcement and concrete, or larger localization error of the major crack. AE in the cells to the right hand side may come from the larger localization error of CR1.

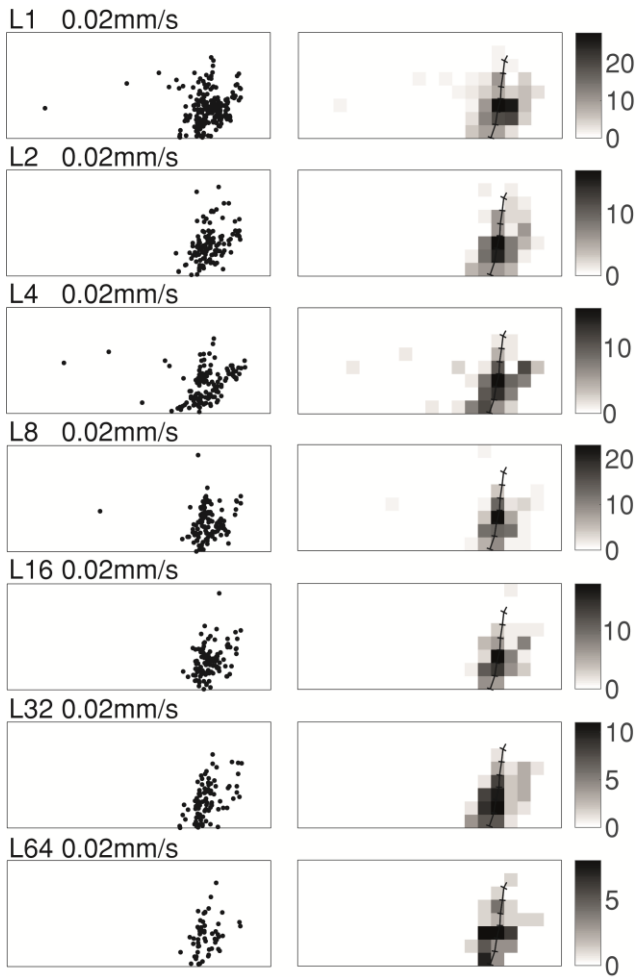


Figure 8. Map of local cumulative AE activities in the selected load cycles in loading Stage 2, with the projected CR2 location. The color bar indicates the local cumulative AE activities.

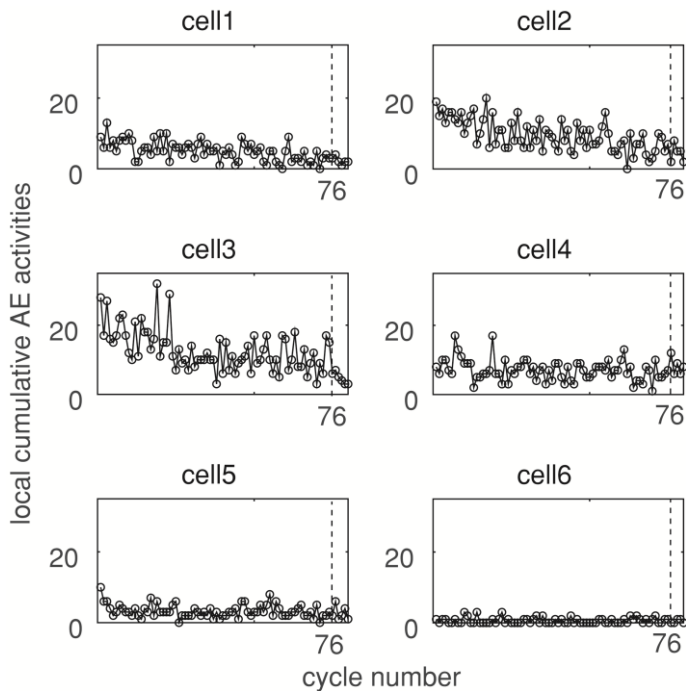


Figure 9. Local cumulative AE activities at cell1-cell6, with dashed line dividing loading Stage 2 (L1-L75) and Stage 3 (L76-L80).

The local cumulative AE activities during unloading in cells 1-6 are particularly shown in Figure 9. In L1, cell2 and cell3 had more cumulative AE activities, which corresponded to the larger local crack closure from DIC results. By comparing L75 to L1, a decrease of local cumulative AE activities was observed in cell2 (from 19 to 7) and cell3 (from 28 to 6). This showed the local smoothing of the crack surfaces.

### Influence of number of load cycles on relationship between local cumulative AE activities and local crack closure

In one load cycle, cells with larger local crack closure generally had more local cumulative AE activities (Figure 8). But, both local cumulative AE activities and local crack closure changed with number of load cycles (Figure 6 and Figure 9, respectively). Therefore, the relationship between local cumulative AE and local crack closure may be inconsistent with increasing number of load cycles.

Figure 10 shows the relationship between local cumulative AE activities and local crack closure in L1 and L75. The arrows indicate the changes in each cell. In L1, local cumulative AE activities significantly increased with local crack closure. But, in L75, local cumulative AE activities were much reduced to values less than 10. They were found not reliable to indicate the local crack closure.

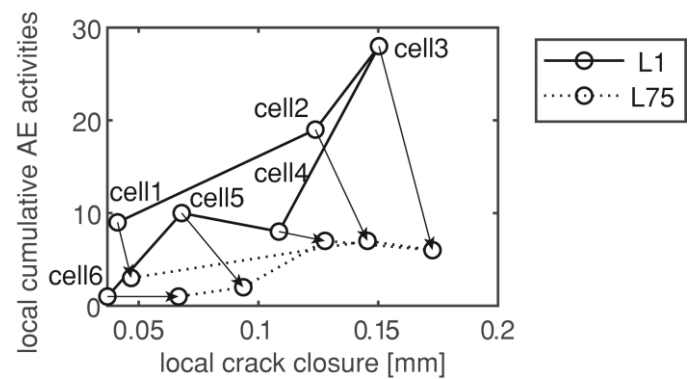


Figure 10. Local cumulative AE activities vs local crack closure in L1 and L75.

### 4.3 Influence of loading speed

After 75 load cycles, in load cycles L76-L80, the influence of number of load cycles was considered insignificant. Comparison of the results in those load cycles can reflect the influence of loading speed on local crack closure and AE-based crack tracking.

### Influence of loading speed on local crack closure

Figure 6 shows that loading speed hardly influenced the local crack closure. Cell3, as an example, had local crack closures of 0.1764 mm, 0.1763 mm, 0.1792 mm, 0.1775 mm, and 0.1723 mm, in L76-

L80 respectively. The difference of the local crack closures was less than 0.01 mm.

### Influence of loading speed on AE-based crack tracking

Little influence of loading speed on the total AE activities was found in Figure 7 (Stage 3).

AE-based crack tracking can still estimate the location of CR2 (Figure 11). A few AE were observed in the un-cracked area. This may due to the closure of micro cracks spread in concrete.

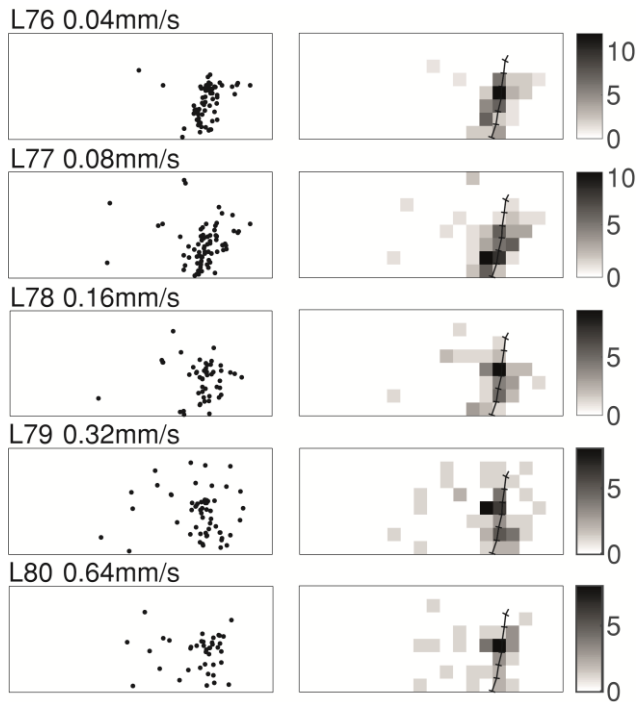


Figure 11. Map of local cumulative AE activities in load cycles in loading Stage 3, with the projected CR2 location. The color bar indicates the local cumulative AE activities.

Local cumulative AE activities changed insignificantly in L76-L80 (Figure 9). Loading speed had little influence on the local cumulative AE activities.

### Influence of loading speed on relationship between local cumulative AE activities and local crack closure

Figure 12 shows the relationship between local cumulative AE activities and local crack closure in L76-L80. Points from a same cell was circled. No clear change was observed in each cell with increasing loading speed. The relationship between local cumulative AE activities and local crack closure was not influenced by the loading speed.

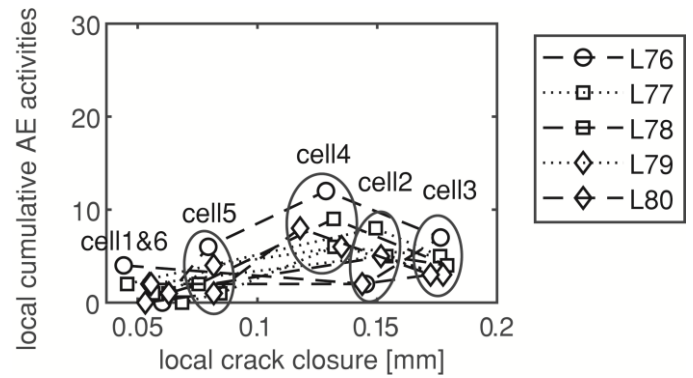


Figure 12. Local cumulative AE activities vs local crack closure in L76-L80, with points from a same cell circled.

## 5 DISCUSSIONS

Based on the study of influence of number of load cycles, we can evaluate the performance of AE-based crack tracking for detecting newly-developed cracks and existing cracks. Newly-developed cracks are referred to cracks that are new with relatively rough crack surfaces. They exist in most lab tests with limited load cycles. Sometimes, new cracks opened during load testing of existing structure, which is not desired for AE-based crack tracking. To evaluate the performance this strategy in detecting newly-developed cracks, AE-based crack tracking in L1 is relevant. For detecting existing cracks, which had smoother crack surfaces, AE-based crack tracking in L75 is more applicable. Cracks in existing concrete bridges are mostly of this type due to the traffic load before the time of test. Comparing AE-based crack tracking in the selected load cycles in L1-L75 (Figure 8) shows that AE-based crack tracking can locate both newly-developed cracks and existing cracks with similar accuracy. But, for existing cracks, AE-based crack tracking had difficulties in indicating the magnitude of local crack closure due to the limited amount of AE activities (Figure 10).

On the other hand, by comparing cracks on their local crack width and local cumulative AE activities, we can distinguish existing cracks and newly-developed cracks. Existing cracks, compared to newly-developed cracks, generally have larger crack width but limited local cumulative AE activities.

Note that local cumulative AE activities depends on many factors, like the selected criteria of AE hits and the size of discretized cells. In this paper, AE hits with peak amplitude over 60 dB were selected. If this criteria was lowered to 50 dB, for example, we would obtain more local cumulative AE activities. Similarly, if the sensor spacing changes, local cumulative AE activities would also change. Therefore, to use the relationship between local cumulative AE activities and local crack closure, a consistent manner of AE-based crack tracking setup is needed.

Load testing of existing bridges may use different loading methods, like loading trucks or hydraulic jets. The loading speed applied on different load testing may not be consistent. Due to the irrelevance to loading speed, AE-based crack tracking for bridges with different loading methods are comparable.

## 6 CONCLUSIONS

This paper investigated the influence of loading protocol including the number of load cycles and the loading speed to AE-based crack tracking performance. The intention was to evaluate the applicability of AE-based crack tracking in existing concrete structures with unknown loading history. Several conclusions can be drawn:

- AE-based crack tracking can indicate the crack pattern, irrelevant to number of load cycles and loading speed.
- By increasing the number of load cycles, the local cumulative AE activities decreased, and the crack closure increased. This results in different relationship between local cumulative AE activities and local crack closure obtained from different load cycles.
- In L1, larger local cumulative AE was related to larger local crack closure. This was more relevant to detecting cracks in most lab tests with limited load cycles.
- In L75, due to the limited local cumulative AE, it is difficult to determine the crack width distribution using AE-based crack tracking. This was more relevant to detecting most cracks in existing concrete structures that underwent many load cycles before the time of test.
- Existing concrete structures may also contain newly-developed cracks. From different relationships between local cumulative AE activities and local crack closure, we can distinguish newly-developed cracks and existing cracks.

## REFERENCE

- EBERL, C. 2010. Digital Image Correlation and Tracking. Mathwork.
- FIB 2003. *Monitoring and safety evaluation of existing concrete structures*, Elsener and Böhni.
- GROSSE, C. & OHTSU, M. 2008. *Acoustic emission testing: Basics for Research-Applications in Civil Engineering*.
- LANTSOGHT, E. O. L., YANG, Y., VAN DER VEEN, C., DE BOER, A. & HORDIJK, D. A. 2017. Beam Experiments on Acceptance Criteria for Bridge Load Tests. *ACI Structural Journal*, 114.
- MISTRAS R6I-AST Sensor. Princeton Junction, NJ 08550: MISTRAS Group Inc.
- MURALIDHARA, S., RAGHU PRASAD, B. K., ESKANDARI, H. & KARIHALOO, B. L. 2009. Fracture process zone size and true fracture energy of concrete using acoustic emission. *Construction and Building Materials*, 6.
- OHTSU, M., UCHIDA, M., OKAMOTO, T. & YUYAMA, S. 2002. Damage assessment of reinforced concrete beams qualified by acoustic emission. *ACI Structural Journal*, 99, 411-417.
- SCHECHINGER, B. & VOGEL, T. 2007. Acoustic emission for monitoring a reinforced concrete beam subject to four-point-bending. *Construction and Building Materials*, 21, 483-490.
- SOUTSOS, M., DENYS, B., GARNIER, V., GONÇALVES, A. & MONTEIRO, A. 2012. Non-Destructive Assessment of Concrete Structures: Reliability and Limits of Single and Combined Techniques.
- ZARATE GARNICA, G. 2018. *Analysis of shear transfer mechanisms in concrete members without shear reinforcement based on kinematic measurements*. Master of Science master thesis, Delft University of Technology.
- ZARATE GARNICA, G. & YANG, Y. 2018. Measurement Report on the Shear Behaviour of 1.2 m Deep RC Slab Strips. Delft: Delft University of Technology.
- ZHANG, F. 2017. *Evaluation of Acoustic Emission Monitoring of Existing Concrete Structures*. Master Master thesis, Delft University of Technology.
- ZHANG, F. & YANG, Y. 2019. Acoustic Emission based Crack Tracking for Existing Concrete Structural Members. *9th International Conference on Acoustic Emission*.